Continuous Extrusion of High-Modulus Semicrystalline Polymers

D. M. BIGG, M. M. EPSTEIN, R. J. FIORENTINO, and E. G. SMITH,
Battelle Columbus Laboratories, Columbus, Ohio 43201

Synopsis

A process has been developed by which very high-modulus semicrystalline polymer films can be extruded continuously from a melt. This is accomplished by controlled cooling of the melt in a two-stage flow channel. A temperature gradient along the flow channel quenches the melt prior to an area reduction in which the polymer undergoes solid-state orientation. Analysis of high-density polyethylene tapes extruded by this process shows that they have properties similar to samples hydrostatically extruded at 120°C. Infrared analysis was used to determine both the degree of crystallinity and degree of orientation in these tapes as well as previously prepared hydrostatically extruded samples.

INTRODUCTION

The tensile strength and modulus of semicrystalline polymers can be substantially increased by solid-state extrusion techniques.[1] Orientation of polymer molecules below the crystalline melting point increases the number of molecules participating in tensile load bearing, thereby increasing the strength and stiffness of the material. Orientation above the melting point is not as effective in increasing the polymer's tensile properties because the molecules possess enough mobility to relax into their thermodynamically preferred spherulitic structures. Solid-state drawing, as used in fiber spinning, is another method for orienting polymer molecules to increase tensile properties. Drawing of shapes other than fibers, however, does not permit the same degree of control over final dimensions that extrusion does. Solid-state extrudates have essentially the same dimensions as the die orifice.

Widespread application of the solid-state extrusion process to polymers has been limited by two principal drawbacks: the batch nature of solid-state extrusion and slow extrusion rates. The conventional way of extruding in the solid state is to mold a solid billet, place the billet in an isothermally controlled chamber, and extrude the polymer through a restriction under the force of a piston. A hydrostatic fluid is frequently employed to reduce extrudate pressure. A sketch of this system is shown in Figure 1. The enhancement of tensile properties is obtained by molecular orientation induced by elongational flow of the polymer through the restriction. The ratio of initial billet area to final billet area is called the extrusion ratio (analogous to draw ratio) and can be directly related to the increase in tensile modulus (see Fig. 2).

In this article a process is described by which solid-state extrusion can be carried out in a truly continuous manner. Some comments regarding extrusion rate limitations are also made.

Journal of Applied Polymer Science, Vol. 26, 395–409 (1981)
 CCC 0021-8995/81/0026-0395$01.50

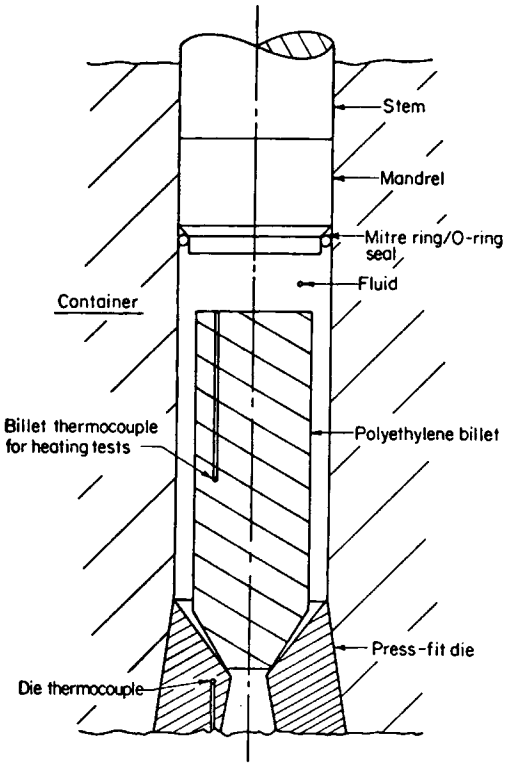

Fig. 1. Sketch of tooling arrangement for hydrostatic extrusion.

EXPERIMENTAL

Process Description

In order to be truly continuous, a polymer process must have a melt consolidation step at some point in the process. The most common melt consolidation device is the screw extruder. This device melts polymeric powders or pellets into a homogeneous mass which is then shaped by a die and quenched into the solid state. In the process described here, a melt is quenched to a temperature just below its melting point while flowing through a cooling channel. The solidified polymer is then forced through a die restriction by the pressure imposed on the melt. When the melt is supplied without interruption, as from a screw extruder, the process is continuous. Because the polymer is solidified when it goes through the die restriction, the tensile properties of the polymer are suitably enhanced. A schematic of the working portion of this process is shown in Figure 3.

Description of Extrusion Apparatus

The major item of tooling constructed for this program is a multiple-piece die designed to extrude HDPE in the form of a thin rectangular tape. The schematic cross-sectional view of the die in Figure 3 shows the essential details of its construction. The upper and lower die sections join to form a continuous, tapered

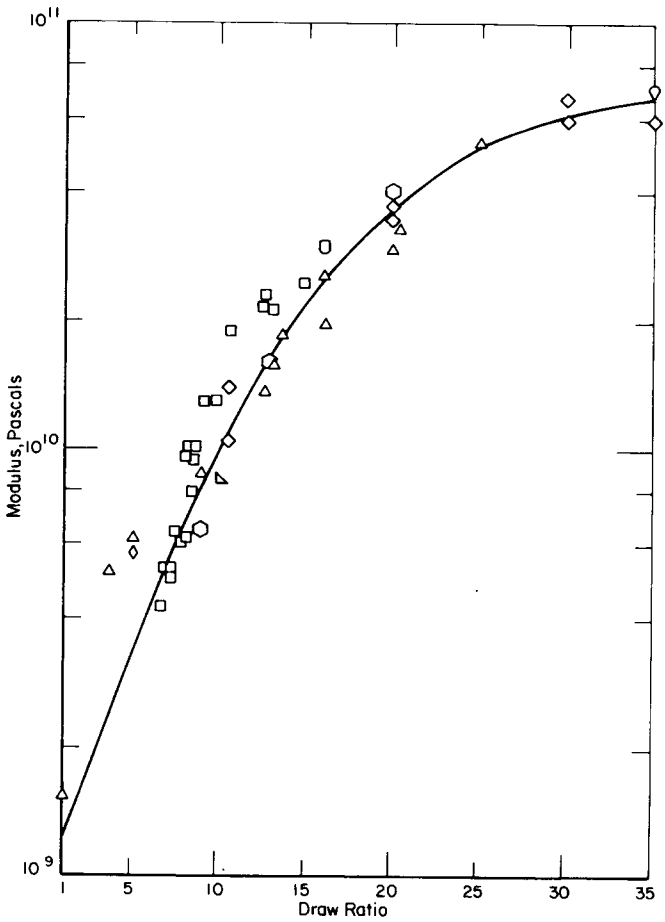

Fig. 2. Tensile modulus as a function of draw ratio for hydrostatically extruded high-density polyethylene (data from ref. 1).

surface that mates with the bore of the extrusion container. Removable inserts fit in the lower die section adjacent to channels through which fluids can be circulated to force-cool the insert.

The upper die section has a conical entry region leading to a flat surface and a rectangular orifice 1.5 mm wide × 25 mm long. This section, with the container bore above it, forms the reservoir where the polymer stock is contained. The rectangular orifice in the upper die section leads to an intermediate cavity (or transition zone) of similar size and shape in the die insert below. Toward the bottom of the cavity, it becomes restricted in width before reaching a smaller orifice. In one insert, the orifice is 0.5 mm wide × 25 mm long, giving a 3:1 extrusion ratio. In a second insert, the orifice is 0.15 mm wide × 25 mm long, resulting in a 10:1 extrusion ratio. Below the insert is a relief opening 3 mm wide × 28 mm long.

In addition to the insert cooling feature, the temperature at several places in the die is measured with thermocouples. Their specific locations are indicated in Figure 3. Thermocouples 1, 2, and 3 are positioned to sense the temperature inside the die components within 1.5 mm of their internal surfaces. Thermo-

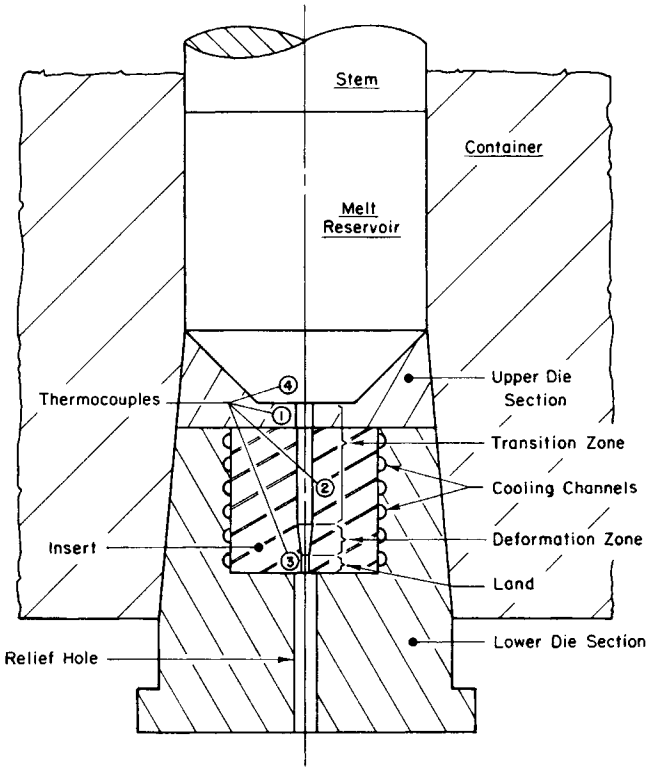

Fig. 3. Cross section of tape die used for continuous extrusion of highly oriented tape.

couple 4 is positioned into the contained bore from above to measure feed stock temperature prior to extrusion, at a distance of 5 mm from the flat surface of the upper die section.

The components of the tape die are shown in Figure 4. The split design of the upper die section (left) and the die inserts (center) can be seen as well as the restricted region of the internal cavity in the disassembled insert. A thin coating of Teflon applied to the interior surfaces of the upper die section and the die insert reduces friction and effectively prevents the HDPE from adhering to these surfaces. The lower die section (right) shows the cooling channels adjacent to the insert cavity and the external lines that feed these channels.

Because a screw extruder that could provide the required extrusion pressures was unavailable at the time this program was conducted, the concept was tested using a hydraulic press to extrude the polymer.

The tape die is mated with a 60-mm bore container installed between platens of a 7-MN vertical hydraulic press. The stem is attached to the upper moving platen which can be operated manually, or at very slow speeds using an adjustable gear-reduction system. Separate cylinders below the press enable the container to be raised and lowered with respect to the die and support tooling mounted on the lower press platen. The cylinders also permit the container to be pulled downward onto the die during an extrusion trial with a force of up to 1 MN. The container and die are heated by resistance heater bands strapped on the outside surface of the container. Power input to the heaters is controlled by a thermo-

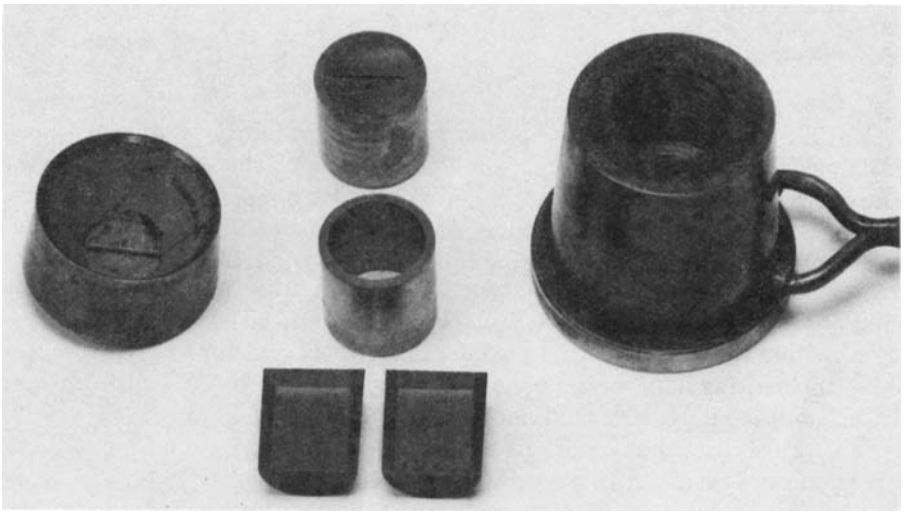

Fig. 4. Extrusion die components showing melt reservoir feed section, area-reducing flow channel, and cooling coils.

couple located in the outer container ring. A feedback system enables a preset temperature to be achieved and maintained in the container.

Materials

The polymer used in this study was Marlex 6009, a high-density polyethylene supplied by Philips Petroleum Company. This polymer has a number-average molecular weight of approximately 9000 and a weight-average molecular weight of 152,000. The polymer has an as-received density of 0.969 g/cm^3, corresponding to a crystalline fraction of 0.70. This was confirmed by DSC measurements. The DSC also determined that the peak melting temperature of the polymer was 133°C. This polymer is reported to have less than two side chains per 1000 carbon atoms.

Procedure

The extrusion runs were made by heating the polymer in the reservoir to a specific temperature, as indicated by thermocouple 4 (see Fig. 3). This produced a natural top-to-bottom temperature gradient of 10–15°C in the die when no forced cooling was used to chill the die. Various degrees of forced cooling produced much larger temperature gradients in the die. Extrusion was initiated by advancing the piston at a fixed rate. A strain gauge mounted in the piston head recorded the extrusion pressure.

The initial runs were made with the 3:1 extrusion ratio insert. Later runs utilized the 10:1 insert. Extruded tape was evaluated for tensile strength and modulus, wide-angle x-ray scattering (WAXS) pattern, and infrared analyses of crystallinity and orientation.

RESULTS

Processing

Continuous lengths of solid tape were extruded under the conditions shown in Table I. Runs 1 through 3 represent trials in which the extrusion ratio was 3:1. For these runs, extrusion was limited to reservoir temperatures above 145°C. Presumably this was because the pressurized polymer solidifed in the reservoir and would not flow into the narrow cooling zone. At reservoir temperatures greater than 155°C, the temperature at the exit of the die was above the melting point of the polymer and melt extrusion occurred. Forced cooling of the die was so severe that the temperature at the inlet to the cooling channel rapidly dropped below the melting point of the polymer. Extrusion was subsequently stopped as the solidified polymer would not flow into the cooling channel.

Table I also lists the conditions used to successfully extrude tape at a 10:1 extrusion ratio. Similar to the results obtained with the 3:1 die, the reservoir–channel conditions were within very narrow limits. Reservoir temperatures higher than 163°C resulted in melt extrusion, while temperatures lower than 155°C caused the polymer to solidify in the reservoir, preventing extrusion. Other parameters, such as extrusion pressure and extrusion rate, are also within narrowly defined limits. Run times as long as 16 hr demonstrated the continuous operation of the process.

Physical Properties

Samples of the 3:1 ratio extruded tape and 10:1 extruded tape (referred to as 3N and 10N respectively) were tested on an Instron tensile tester at 0.127 cm/min. The results are shown in Table II, where they are compared to the unoriented polymer and a sample produced in a previous study.[2] The previously produced sample was hydrostatically extruded at 120°C at an extrusion ratio of 13:1. This sample is designated 13N. In an earlier report it was shown that a relationship exists between tensile modulus and isothermal solid-state orientation.[1] This relationship is shown in Figure 5 for high-density polyethylene. Sample 3N, having a nominal extrusion ratio of 3:1, fits the empirical curve quite well. The modulus of sample 10N has a higher modulus than would be expected from polyethylene extruded at a 10:1 extrusion ratio. The tensile strength and elongation to break are also indicative of orientation greater than would be ex-

TABLE I
Summary of Extrusion Conditions[a]

Run No.	Extrusion ratio	Reservoir temp., °C	T_1, °C	T_2, °C	T_3, °C	Extrusion pressure, MPa	Extrusion rate, mm/min	Run time, hr
1	3	145	135	123	116	25	5	0.5
2	3	149	139	132	127	50	10	0.25
3	3	155	144	138	134	25	25	0.50
4	10	157	144	139	134	60	15	16
5	10	159	145	139	133	65	15	14
6	10	163	146	140	135	75	10	0.5

[a] Subscripts in T_1, T_2, and T_3 refer to thermocouple position in Figure 3.

TABLE II
Summary of the Physical Properties of Oriented Polyethylene

Sample No.	Tensile strength, MPa	Tensile modulus, GPa	Elongation to break, %
Unprocessed	29.7	1.70	600.0
3N	65.9	2.58	21.0
10N	450.0	16.80	8.7
13N	420.0	13.40	12.0

pected at a 10:1 extrusion ratio. These properties show evidence of equal, or slightly greater, orientation in sample 10N when compared with sample 13N.

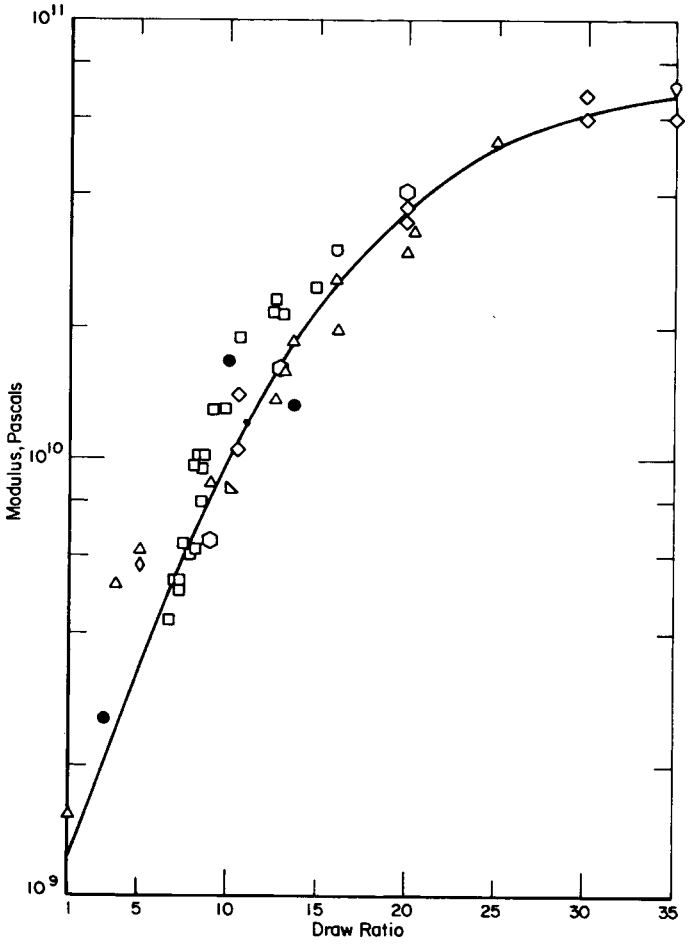

Fig. 5. Comparison of extruded tape moduli with prior modulus draw ratio data. Filled data points are from this program, while open data points are from ref. 1.

WAXS Patterns

Wide-angle x-ray scattering (WAXS) photographs were taken normal to the film plane of samples 3N, 10N, and 13N and are shown in Figure 6. The direction of orientation was along the vertical plane. Randomly oriented crystalline polymers produce a WAXS picture containing concentric circles representing each of the possible lattice planes. As the polymer is oriented, the lattice planes will reflect the x-rays at a specific angle. On the WAXS photograph this shows up as a series of arcs at specific polar locations.[3] The smaller the arc length, the greater the degree of orientation. Figure 6(a) shows that sample 3N is only slightly oriented since the arcs are quite long. The arcs for sample 10N and 13N are very short, however, indicating a high degree of orientation. The arcs on the horizontal plane represent c-axis, or molecular chain, orientation. This degree of orientation is approximately equal for samples 10N and 13N.

Infrared Analysis of Degree of Orientation

Infrared analysis was also used to evaluate orientation. From parallel and perpendicular polarized infrared spectra, the dichroic ratio of the 1894 cm^{-1} band can be used to determine Hermans orientation function f_c.[4] The subscript refers to the fact that the c-axis or main chain axis orientation is being compared to the macroscopic orientation direction. The 1894 cm^{-1} band arises only from CH_2 rocking in the crystalline phase. The dichroic ratio is simply

$$D = \frac{A_\parallel}{A_\perp} \tag{1}$$

where A is the absorbance of the band of interest. According to Fraser,[5]

$$f_c = \frac{(D-1)(D_0+2)}{(D+2)(D_0-1)} \tag{2}$$

where

$$D_0 = 2\cot\phi \tag{3}$$

and ϕ is the angle between the chain axis and the direction of the transition moment. Theoretically, ϕ is 90° for linear polyethylene. Experimentally, it has been determined to be between 87° and 89°.[6] D_0 is, therefore, insignificant in evaluating f_c, which represents the fraction of perfectly oriented chains in the

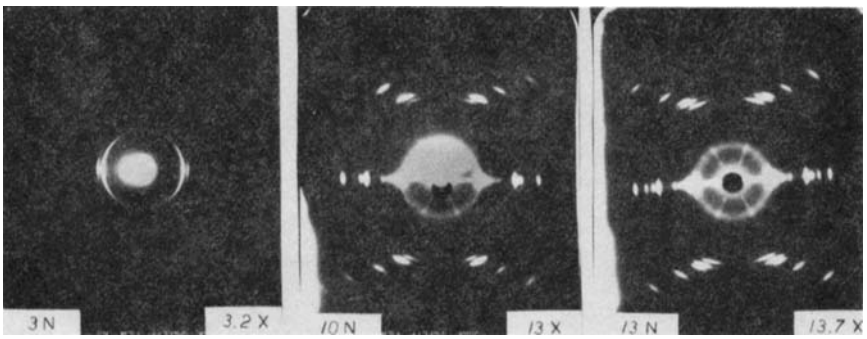

Fig. 6. WAXS patterns for samples 3N, 10N, and 13N.

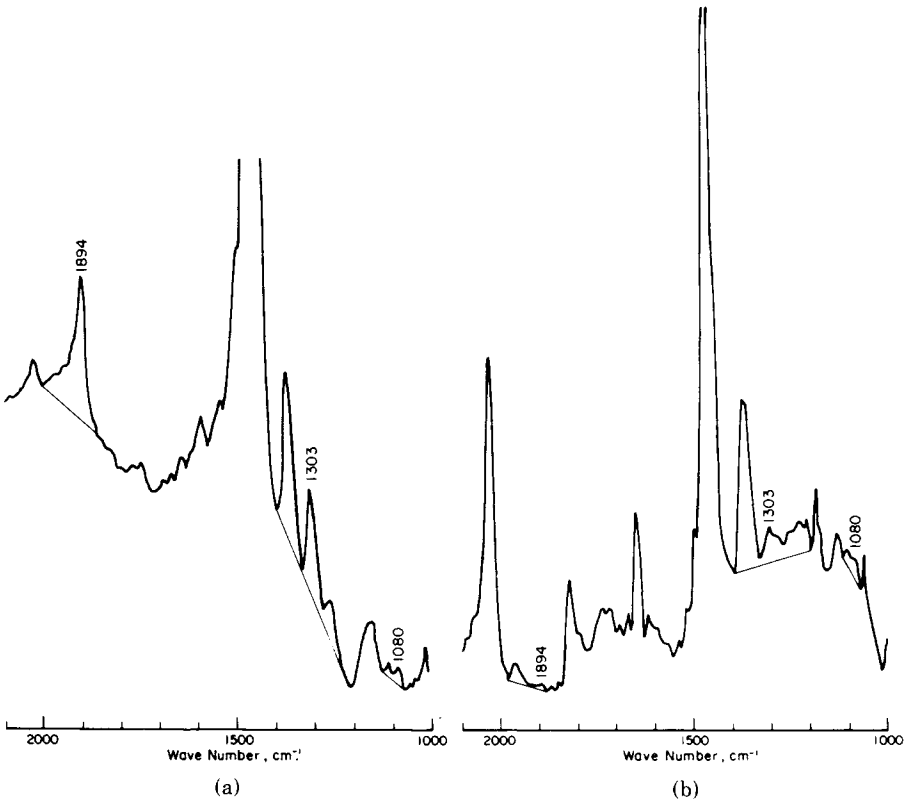

Fig. 7. Infrared absorption spectra for sample 10N: (a) perpendicularly polarized; (b) parallel polarized.

crystal lattice. A fully oriented polymer would have a value of f_c equal to 1. It does not reflect the degree of crystallinity, chain fold lengths, or amorphous-phase orientation. Knowing f_c, the average angle $\bar{\theta}$ between the chain axis and the draw direction can be calculated as

$$\bar{\theta} = \left[\cos^{-1}\left(\frac{2f_c + 1}{3}\right)\right]^{1/2} \tag{4}$$

Figure 7 shows the polarized infrared spectra in the 1000–2100 cm^{-1} band region for sample 10N. The appropriate baselines for measuring absorbancies are also shown. Table III summarizes the results of various orientation parameters determined from these spectra. Clearly, the crystals are more highly aligned to the extrusion direction for samples 10N and 13N than for sample 3N. This was expected, since the nominal extrusion ratio was considerably higher

TABLE III
Summary of Orientation Parameters of Extruded Samples

Sample No.	$A_{\parallel}^{1894}$	$A_{\perp}^{1894}$	D^{1894}	$\bar{\theta}$	f_c
3N	0.075	0.260	0.288	30.1	0.622
10N	0.005	0.950	0.0526	13.1	0.923
13N	0.020	0.370	0.054	13.3	0.921

and the WAXS photograph showed much more orientation. Samples 10N and 13N have almost identical orientation functions. This supports the indications given by the WAXS pictures. Evidently, sample 10N was oriented to a degree greater than expected by the 10:1 area reduction. It appears that some orientation developed while the material flowed from the melt reservoir into the cooling channel which did not completely relax prior to freezing. Because of the relatively low temperatures used in the process, this proposition is very likely.

Determination of Degree of Crystallinity

The properties of semicrystalline polymers depend strongly on the degree of crystallinity of the material. Various techniques are available to determine the crystalline fraction of a polymer. Unfortunately, some of these techniques are influenced by the degree of orientation. Measurement of percent crystallinity by infrared analysis has been reported to be independent of the degree of orientation.[7] As shown by Hendus and Schnell,[8] the fractional crystallinity χ can be obtained from the ratio of absorbancies of the 1894 cm^{-1} bands:

$$\chi = \frac{A^{1894}/A^{1303}}{(A^{1894}/A^{1303}) + (K/A)} \tag{5}$$

where A and K are extinction coefficients for completely amorphous and completely crystalline polyethylene. K was determined to be 6.1 cm^{-1}, and A was measured as 17 cm^{-1}. Absorption values can be obtained from polarized infrared spectra from the following relationship for unaxially oriented polymers:

$$A = \tfrac{1}{3}(A_{\parallel} + 2A_{\perp}) \tag{6}$$

Differential scanning calorimetry (DSC) provides not only fractional crystallinity but melting point, melting range, and heat of fusion. The effect of orientation on DSC measured crystallinity is unknown. X-Ray techniques are also used to determine fractional crystallinity,[9] although this method has been shown to be sensitive to orientation.[10] Table IV summarizes the data obtained by x-ray, IR, and DSC measurements of crystallinity. The x-ray results, as expected, are clearly much too high. The infrared measurements are an average of 3.3% lower than the DSC measurements of fractional crystallinity. The differences in crystallinity between the three oriented samples are most likely due to different thermal histories than to degrees of orientation. Glenz and Peterlin showed that the degree of crystallinity changes in an unexpected manner in isothermal orientation.[7] The relationship between fractional crystallinity and draw ratio was very dependent on prior thermal history. The different thermal

TABLE IV
Summary of Crystalline Properties Measured by X-Ray and DSC Techniques

Sample No.	χ DSC	χ IR	χ X-Ray	T_m, °C	ΔH_{fus}, cal/g
Unprocessed	0.696	—	—	133	47.6
3N	0.740	0.723	0.850	133	50.8
10N	0.780	0.767	0.960	137	53.6
13N	0.840	0.800	—	137	58.1

histories of samples 10N and 13N account for the large difference in fractional crystallinity, even though these two samples are oriented to about the same degree.

The melting temperatures of samples 10N and 13N are also the same, 137°C. The increase in melting point is a result of the longer fold length and more highly ordered crystalline structure of these highly oriented samples. For sample 3N, which has a low degree of orientation, the melting point is unchanged from that of the isotropic polymer. Figure 8 shows that although the melting point of sample 3N is the same as that of the unoriented polymer, the melting endotherm is narrower and the degree of crystallinity greater. The narrowness of the melting endotherm results from the increased order of the oriented crystals. The melting endotherm of sample 10N is similarly narrow, indicating a high degree of crystalline order.

DISCUSSION OF RESULTS

The feasibility of continuously extruding high modulus polyethylene tape in the solid state has been demonstrated. With the die used in this program, a narrow range of conditions was found which would satisfy the requirements of

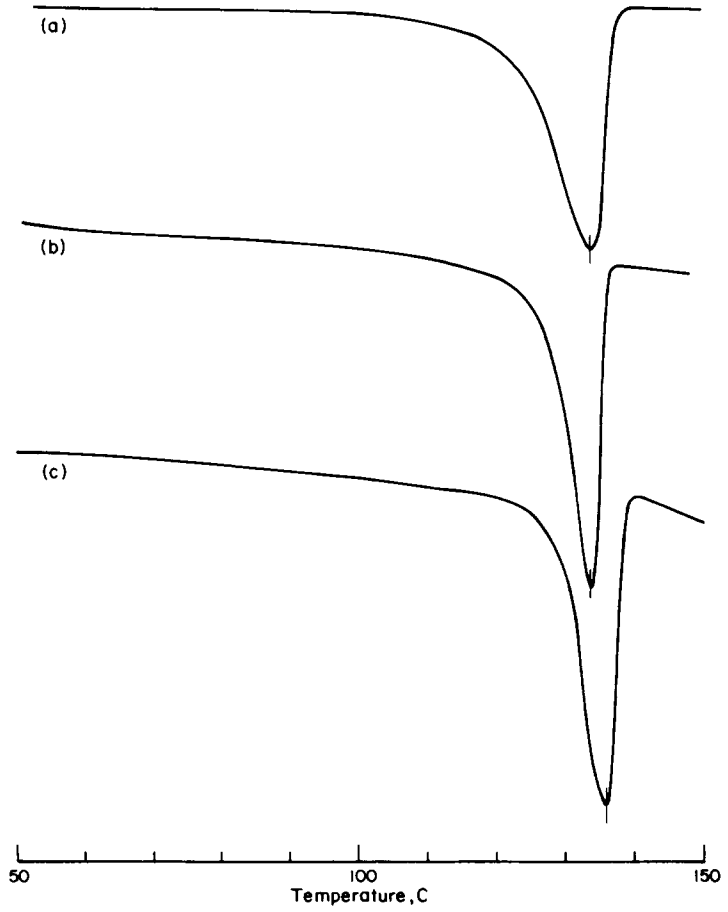

Fig. 8. DSC curves of (a) unoriented polyethylene, (b) sample 3N, and (c) sample 10N.

a fluid polymer in the reservoir and a solid polymer in the cooling channel just prior to the area reduction. Because the required extrusion pressures were approximately 25 MPa for the 3:1 reduction and 75 MPa for the 10:1 reduction, the melting point of the polyethylene in the reservoir was increased 8 and 11°C, respectively.[11] The respective melting points at 25 and 75 MPa are 141 and 154°C. Extrusion was possible only when the reservoir temperature was above the elevated melting point of the polymer.

Forced cooling of the die reduced the cooling channel and reservoir temperatures well below the melting point of the polymer. The use of heated water or oil reduced the temperature drop in the die but did not allow a suitable temperature gradient to be established in the die. A different die design would permit a specified temperature gradient rather than the natural gradient that developed. The natural gradient was caused by heat losses through the die into the atmosphere. This gradient was typically 10–15°C along the die. Reservoir temperatures were also 10–15°C greater than the temperature at the top of the cooling channel. Figure 9 shows the temperature profile of the polymer and cooling channel wall for run 5 of Table I. This plot shows that the polymer reaches the wall temperature prior to the entrance of the area restriction. Details

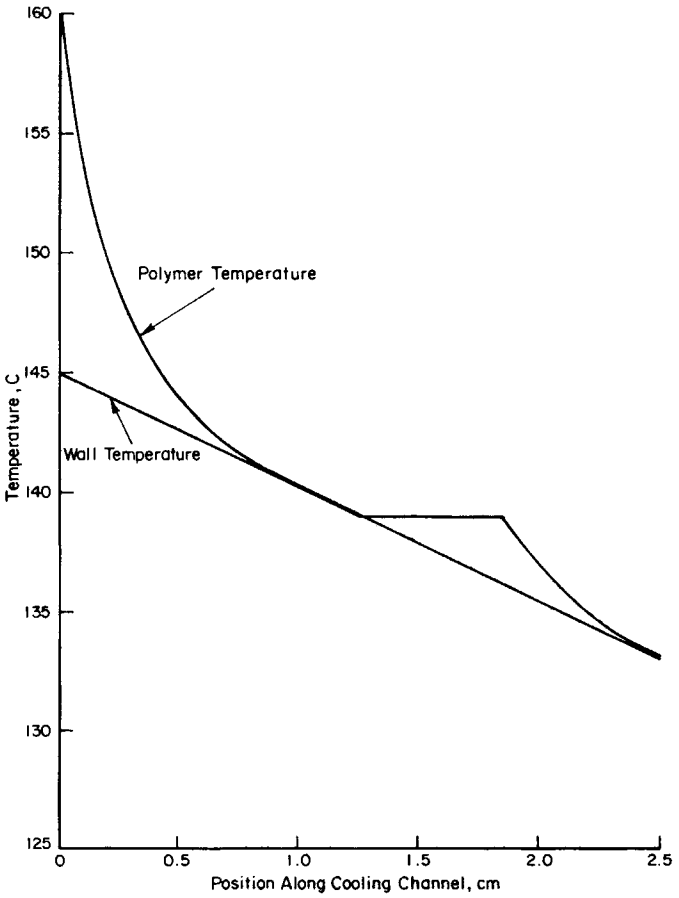

Fig. 9. Calculated temperature profile in the cooling channel.

of the calculation of the profile are given in the Appendix. As long as the polymer temperature is below 133°C at the die restriction, solid-state orientation will occur. It is clear that the natural temperature gradient accomplishes this as long as the reservoir temperature is below 160°C. With the die used in this project, reservoir temperatures were limited to between 145 and 160°C.

The effect of extrudate rate on the temperature profile was not determined. Theoretically, a faster rate would add heat to the die, reducing the temperature to maintain the polymer below 134°C at the die restriction. In turn, the lower reservoir temperature would increase the extrusion pressure and possibly induce flow instability. Ideally, the die should have independent cooling to accommodate higher extrusion rates. The maximum extrusion rate will depend on the stability of the polymer flowing through the restriction at a temperature just below the melting point. It has been shown by several research groups that the maximum rate of hydrostatic extrusion is limited by the extrudate distortion.[12–15]

The enhancement of the tensile modulus and strength also indicates that the polymer was in the solid state while being oriented in the die restriction. Evidence from the modulus, WAXS pattern, and infrared determination of f_c indicates that the orientation imparted to the polymer during flow in the 10:1 area reduction die is greater than would be expected from isothermal hydrostatic solid-state extrusion. Comparisons of the tensile modulus, WAXS pattern, and f_c between samples 10N and 13N reveal that both samples were oriented to approximately the same degree. Sample 13N was extruded isothermally and has properties similar to those expected from polyethylene extruded in the solid state at a 13:1 extrusion ratio. Because sample 10N was nominally extruded through only a 10:1 area reduction, some orientation was induced in the cooling channel. This is not unreasonable, since some orientation is induced in injection-molded samples. This is beneficial in that a lower area reduction can be used to obtain a desired degree of orientation. This results in lower extrusion pressures and higher extrusion rates.

This work was sponsored by Brookhaven National Laboratories under the helpful guidance of Mr. Al Muller.

APPENDIX

Determination of Cooling of Polymer in Cooling Channel

From ref. 16, the cooling of a film can be expressed as

$$\frac{T - T_w}{T_0 - T_w} = e^{-2hz/\rho C_p U W} \tag{A-1}$$

where T is the polymer temperature at z, T_w is the temperature of the die wall, T_0 is the reservoir polymer temperature, h is the heat transfer coefficient between the polymer and wall, z is the length down the cooling channel, ρ is the polymer density, C_p is the polymer specific heat, U is the linear flow velocity of the polymer, and W is the channel width.

This equation assumes that the polymer has no thickness temperature profile. Separate calculations showed that cross-sectional temperature variations were negligible. The values of all the parameters used in the calculations are listed in Table A-I. h was determined from ref. 17 as

$$h = \frac{Nuk}{2B} \tag{A-2}$$

TABLE A-I
Values Used in Determining Cooling Curve

ρ	Polymer density; melt = 0.86 g/cm^3, solid = 0.96 g/cm^3
C_p	Polymer specific heat = 0.55 cal/g °C
U	Linear velocity of polymer = 0.0083 cm/sec
W	Channel width = 2.54 cm
B	Channel thickness = 0.15 cm
k	Polymer thermal conductivity = 0.001 ca/sec cm °C
λ	Latent heat of fusion, 50 cal/g

where Nu is the Nusselt number, k is the thermal conductivity of the polymer, and B is the thickness of the cooling channel.

For Newtonian flow, which is a valid assumption because of the very slow flow, Nu is 7.54.[17] Therefore, for the 0.015-cm-thick tape,

$$h = \frac{(7.54)(10^{-3})}{(2)(0.15)} = 0.25 \text{ cal/sec cm}^2 \text{ °C}$$

Experimental data from run 5 give the following wall temperature profile:

$$T_w = 145 - 4.8z \tag{A-3}$$

For the cooling of the melt prior to solidification, eq. (A-1) becomes, upon substitution of the appropriate values,

$$T = 145 - 4.8z + (15 + 4.8z)e^{-5z} \tag{A-4}$$

The melting point of high-density polyethylene at 100 MPa pressure is 154°C.[11] The crystallization temperature upon cooling is 15°C below the melting point and is 139°C. Equation (A-4) is valid until T reaches 139°C. At this point, the polymer moves as a plug, and the Nusselt number and density change. There is also a delay in polymer temperature drop as the latent heat is removed. Heat transfer in the freezing zone is given by

$$Q = hA\Delta T \tag{A-5}$$

where

$$\Delta T \approx \frac{\Delta T(\text{initiation of freezing}) + \Delta T(\text{end of freezing})}{2} \tag{A-6}$$

When eq. (A-4) is plotted, it is shown that the polymer temperature reaches that of the wall in approximately 1 cm (Fig. 9). Therefore, ΔT(initiation of freezing) is approximately zero. At the end of freezing,

$$\Delta T = 139 - (145 - 4.8z_e) = 4.8z_e - 6$$

where z_e is the position where freezing is complete. For plug flow, the Nusselt number is 9.86[17] such that

$$h = \frac{(9.86)(10^3)}{(2)(0.15)} = 0.033 \text{ cal/sec cm}^2 \text{ °C}$$

Equation (A-5) becomes

$$Q = \frac{(0.033)(2)(2.54)(z_e - z_i)(4.8z_e - 6)}{2}$$

where z_i is the point where freezing is initiated. From Figure 9 this is when z equals 1.25 cm. Therefore,

$$Q = 0.4z_e^2 - z_e + 0.63 \tag{A-7}$$

Q is the amount of heat removed to melt the polymer and can be calculated from

$$Q = \rho BWU\lambda \tag{A-8}$$

Substituting in the numerical values gives

$$Q = (0.0083)(0.96)(2.54)(0.15)(50) = 0.152 \text{ cal/sec}$$

Equation (A-7) now becomes

$$z_e^2 - 2.5z_e + 1.2 = 0 \tag{A-9}$$

The positive solution to eq. (A-9) is $z_e = 1.85$ cm. Cooling now proceeds according to eq. (A-1) with T_0 now equal to 139°C and ρ that of the solid polymer. This equation becomes

$$T = (145 - 4.8z) + (4.8z - 6)e^{-5.9(z-1.85)} \tag{A-10}$$

The complete cooling curve is shown in Figure 9. This curve shows that the polymer quickly reaches the temperature of the wall and freezes before the area constriction. It also shows that the polymer temperature prior to area reduction under these conditions is 133°C, just below the ambient melting point of the oriented polymer, 137°C.

References

1. D. M. Bigg, *Polym. Eng. Sci.*, **16,** 725 (1976).
2. D. M. Bigg, M. M. Epstein, R. J. Fiorentino, and E. G. Smith, *Polym. Eng. Sci.*, **18,** 908 (1978).
3. R. J. Samuels, *Structured Polymer Properties,* Wiley, New York. 1974.
4. I. M. Ward, *Structure and Properties of Oriented Polymers,* Wiley, New York, 1975.
5. R. D. B. Fraser, *J. Chem. Phys.*, **24,** 89 (1956).
6. B. E. Read and R. S. Stein, *Macromolecules,* **1,** 116 (1968).
7. W. Glenz and A. Peterlin, *J. Macromol. Sci. Phys.*, **4**(3), 473 (1970).
8. H. Hendus and G. Schnell, *Kunstoffe,* **51,** 69, (1961).
9. P. Meares, *Polymers: Structure and Bulk Properties,* Van Nostrand, London, 1965.
10. M. A. McRae, W. F. M. Addams, and J. E. Preedy, *J. Mater. Sci.*, **11,** 2036 (1976).
11. R. N. Gupta, P. C. Jain, V. S. Nanda, and A. S. Reshamwala, *J. Appl. Polym. Sci.*, **21,** 2621 (1977).
12. J. M. Alexander and P. J. H. Wormell, *Ann. C.I.R.P.*, **19,** 21 (1971).
13. K. Nakayama and H. Kanetuswa, *Kobunshi Ronbunshu, Eng. Ed.*, **2,** 1009 (1973).
14. L. A. Davis, *Polym. Eng. Sci.*, **14,** 641 (1974).
15. H. N. Yoon, K. D. Pae, and J. A. Sauer, *Polym. Eng. Sci.*, **16,** 567 (1976).
16. S. Middleman, *Fundamentals of Polymer Processing,* McGraw-Hill, New York, 1977, p. 399.
17. R. B. Bird, R. C. Armstrong, and O. Hassager, *Dynamics of Polymeric Liquids,* Vol. 1, Wiley, New York, 1977, p. 237.

Received March 25, 1980
Accepted May 22, 1980